Greenhouse gas flux studies: An automated online system for gas emission measurements in aquatic environments

Nguyen Thanh Duc[1,4], Samuel Silverstein[2], Martin Wik[3], Patrick Crill[3], David Bastviken[4], Ruth K. Varner[1]

[1]Institute for the Study of Earth, Oceans and Space and Department of Earth Sciences, University of New Hampshire, Durham, 03824, USA
[2] Department of Physics, Stockholm University, 106 91, Sweden
[3] Department of Geological Sciences, Stockholm University, 106 91, Sweden
[4]Department of Thematic Studies - Environmental Change, Linköping University, 581 83, Sweden

Correspondence to: Nguyen Thanh Duc (thanh.duc.nguyen@liu.se)

Abstract. Aquatic ecosystems are major sources of greenhouse gases (GHG). Robust measurements of natural GHG emissions are vital for evaluating regional to global carbon budgets and for assessing climate feedbacks on natural emissions to improve climate models. Diffusive and ebullitive (bubble) transport are two major pathways of gas release from surface waters. To capture the high temporal variability of these fluxes in a well-defined footprint, we designed and built an inexpensive device that includes an easily mobile diffusive flux chamber and a bubble counter, all in one. In addition to automatically collecting gas samples for subsequent various analyses in the laboratory, this device also utilizes a low cost carbon dioxide (CO_2) sensor (SenseAir, Sweden) and methane (CH_4) sensor (Figaro, Japan) to measure GHG fluxes. Each of the devices were equipped with an XBee module to enable a local radio communication (DigiMesh network) for time synchronization, and data readout at a server-controller station on the lakeshore. Software of this server-controller is operated on a low-cost computer (Raspberry Pi) which has a 3G connection for remote control and monitor functions from anywhere in the world. This study shows the potential of a low cost automatic sensor network system to study GHG fluxes on lakes in remote locations.

1 Introduction

Despite the fact that lakes and impoundments only cover around 3.7% of the continental area (Downing et al., 2006;Verpoorter et al., 2014), their contribution to global carbon dioxide (CO_2) and greenhouse gas (GHG) budgets are substantial (Tranvik et al., 2009; Bastviken et al., 2011; Raymond et al., 2013). Lake emissions are not only large, but previous studies also highlight large uncertainties in overall emission estimates. For example, a recent synthesis of CH_4 emissions from northern lakes and ponds reveals that these aquatic environments contribute 16.5 Tg CH_4 yr^{-1}, equivalent to more than 65% of inverse model calculation of all natural CH_4 sources in the region where CH_4 fluxes were believed to be largely emitted from wetlands (Wik et al., 2016b). In addition, the climate sensitivity of the natural emissions are important and unclear, but metadata analyses showed that CH_4 emission and the ratio of CH_4 to CO_2 emissions increase markedly with the increasing temperature (Yvon-Durocher et al., 2014; Marotta et al., 2014). However, previous field studies of these greenhouse gases emissions are still limited in their spatial and temporal resolution, which potentially result in low quality measurements and biased estimates (Wik et al., 2016a). For this reason, there is a need for more efficient tools to study the emission of CH_4 and CO_2 from open, fresh water ecosystems at both higher temporal and spatial resolutions.

Using conventional techniques with well-defined footprints, emitted gases are trapped in air-filled flux chambers (FC) or submerged water-filled funnels (Chanton and Whiting, 1995). When properly designed, the flux chamber method which can trap both diffusive and ebullitive (bubble) fluxes, has been demonstrated to not bias gas fluxes at the air-water interface relative to SF_6 assessments (Cole et al., 2010) or other independent methods(Gålfalk et al., 2013; Lorke et al., 2015). The submerged funnel is specifically used to trap bubbles (Wik et al., 2013). The trapped gas in chambers or submerged funnels

is commonly collected manually with syringes after a practical time interval, and analyzed in the laboratory. Both these methods are inexpensive in terms of equipment and work well to quantify gas emission in a confined area but they are labor intensive and have low temporal resolution. During short term measurements, there is also a high probability of missing ebullition events. During long term chamber or funnel deployments, CH_4 dissolution and or oxidation in the water that is in
5 contact with the trapped gas could result in an underestimation of flux. Most previous measurements were based on infrequent measurements within short time frames (0.5 to 24 hrs) and likely did not capture ebullition in a representative way thereby resulting in underestimation (Wik et al., 2016a). As a result, there is a high uncertainty in extrapolations and modeling of CH_4 and CO_2 emissions over time (Smith, 1985; Walter et al., 2001; Bastviken et al., 2004; Meng et al., 2012). High frequency measurements over long periods with broad spatial coverage of studied areas could reduce this uncertainty
10 and result in more representative gas emission estimates. Regarding the floating chamber approach, there are automated methods in which the trapped gases in the chamber can be sampled with a system of pipes and large pumps connected to a gas analyzer (Goodrich et al., 2011; Goulden and Crill, 1997). This can better address the temporal variability, but the gas analyzer equipment is typically expensive. The chambers also need to be relatively close to the gas analyzer so this method can be limited in spatial coverage. Some recent studies using low cost CH_4 (Eugster and Kling, 2012) and CO_2 sensors
15 (Bastviken et al., 2015) could however be coupled to simultaneously study CH_4 and CO_2 flux across the air-water interface.

Carbon dioxide flux measurements require a short time period for chamber deployment due to rapid equilibration. There are commercially available high precision CO_2 sensors available (e.g: Li-Cor, Vaisala-CO_2)(Johnson et al., 2010; Anderson et al., 1999) which can be connected to chambers for CO_2 analysis. However, their cost makes it difficult to afford many
20 simultaneous measurements across a study area. Recently, Bastviken *et al.* (2015) proposed the use a low-cost CO_2 sensor and developed applications for pCO_2 and CO_2 flux measurement in outdoor environments.

Other techniques based on video/photo or hydro acoustic methods have been developed to evaluate the time and place of
25 ebullition (Ostrovsky et al., 2008; Tassin and Nikitopoulos, 1995). The acoustic method has a high potential for solving the spatial heterogeneity of gas emission, but this technique has a high cost regarding the equipment combined with some uncertainties in quantifying gas emissions. In addition, this technique may work well in ecosystems with frequent ebullition, but sonar scanning is time and power consuming over extended periods in ecosystems where ebullition is less frequent. In such systems, there is a need for inexpensive and power-efficient equipment for long term, continuous monitoring of
30 ebullition. Varadharajan et. al (2010) published a low-cost automated trap to measure ebullition flux using an inverted funnel connected to a pressure sensor whose signal was recorded by a commercial data logger. This type of commercial data logger and funnel requires manual maintenance and gas release, and there are risks of missing ebullition events when the trap is full of gases. The eddy covariance (EC) technique is increasingly used for long-term monitoring, but it is expensive in terms of equipment and is still being evaluated for aquatic environments. In addition, such measurements cannot account for spatial
35 variability within the footprints of the EC measurement.

To increase the quality and quantity of observations of aquatic GHG emission, we developed a low-cost, simple, robust and portable device with a well-defined footprint for investigating gas flux at the water-air interface. This is a follow up from our previous open-tech published work about measuring CH_4 by an AFC (Duc et al. 2013), now substantially improved by
40 including sensors to reduce the need of laborious manual sampling and analyses, a wireless on-line readout-control device that has the capability to simultaneously measure ebullitive fluxes by an automatic bubble counter (ABC) and diffusive CH_4, CO_2 fluxes by an automatic floating chamber. Taking advantage of small, low cost CH_4 and CO_2 sensors, we have modified our automated flux chamber (AFC), which is composed of a flux chamber connected to an automated control box (Duc et al., 2013), to measure CH_4 and CO_2 flux from aquatic environments. The CH_4 sensor tested here is a Taguchi Gas Sensor (TGS)
45 (Figaro Engineering Inc., Osaka, Japan). It is a high sensitivity CH_4 gas sensor made for air contaminants and gas leak detection. Eugster and Kling (2012) showed that this sensor has potential to measure CH_4 at ambient air concentrations. The sensor has a high sensitivity to relative humidity and temperature, but these responses can be corrected for to yield a realistic CH_4 signal. Here, we test three commercial sensors including: TGS2611-E00, NGM 2611-E13, and a Panterra CH_4 sensor. The TGS2611-E00 sensor is equipped with a filter to reduce the influence of interference gases, resulting in a selective
50 response to CH_4. The NGM 2611-E13 is a pre-calibrated module which is also based on the sensor TGS2611. This module is

prebuilt as a gas detector circuit and has been calibrated in Figaro's humidity and temperature controlled facility. The Panterra CH_4 sensor (PN-SM-GMT-A040A-W20A-05-R0- S0-E1-X0-I2-P0-L2-J1-Z0, Panterra Neodym Technologies, Canada) which is based on a TGS2610 sensor, and has been pre-calibrated by the manufacturer. The CO_2 sensor used here (CO_2 Engine ELG K33, from SenseAir, Sweden) is a low-power module that measures CO_2, temperature and relative

5 humidity. Therefore, this CO_2 sensor can provide temperature and humidity data to correct the CH_4 sensor response. The sensor equipped AFCs were combined with submerged funnels for automated detection of bubbles. Here, we suggest a solution to automatically collect or release the trapped gas, and restart the bubble trap by using a pump and valve system, which are controlled by an inexpensive microcontroller-based data logger, based on the feedback of the pressure signal.

2. Methods

10 In this section, we describe the technical details of our new device that simultaneously measures CH_4 ebullition, diffusive CH_4 emissions, CO_2 flux and equipped the system with a radio transmitter module for wireless data transfer and monitor. The system consists of a floating control box housing the electronics, a floating chamber and a submerged funnel. The control box is a watertight case which stores a power source (either a 12V 7Ah lead-acid battery or a 12V 55Ah lithium ion battery (Power Pack LS 55, vuphongsolar.com, Vietnam inside and a solar panel mounted on the top of the box), diaphragm

15 pumps, electronic valves, a pressure sensor and the electronic controller boards. The control box connects to either the chamber or the funnel or both of them. Compared with the previous version in Duc et al. (2013), the electronic controller boards, including the power control board and the data logger board, have been redesigned to include an open 5Vdc supply for a CH_4 sensor, an open I2C connection for a CO_2 sensor, and an open UART2 connection for XBEE radio communication.

20 2.1 Ebullition counter

Using an inverted funnel design (Wik et al., 2013) to selectively capture ebullition, we developed an inexpensive automated bubble counter (ABC) which adopted the measurement principle of the low cost automated trap of Varadharajan et. al (2010). From the funnel stem, a 30-cm PVC pipe (10 mm I.D.) was attached to accumulate bubbles. The other end was attached to an inverted 10 mL syringe whose tip was connected to a pressure sensor via a polyurethane tube (Figure S1). Gas

25 accumulating in the pipe pushes down the water level relative to the water level outside the pipe, and this water level difference generates a pressure that is proportional to the gas volume in the pipe. Ebullition (mL) is determined from the differential pressure inside the pipe over time; therefore, it is important to make the trap gas tight.

The ABC is a part of an automatic measurement device which can be programed to simulate the deployment cycle of a
30 manual trap including capturing bubbles and releasing of gases when trap is full. To enable autonomous operation for long deployment periods, a pressure sensor and a pump and a 2-way valve were connected to the bubble trap with a 3.175 mm inner diameter polyurethane tube (Clippard URT1-0805) and two T-connectors (Figure S1). The pump and valve were powered by 12Vdc. The pressure sensor was power by regulated 10Vdc; its signal was amplified 495-fold by an AD620 chip (Analogue Devices; USA).
35

The microcontroller-based datalogger board continuously reads the amplified pressure sensor signal, and a step-wise pressure increase from gas accumulation indicates an ebullition event that is recorded with date and time stamps. The bubble measuring cycle of the ABC in the field includes initiation, measurement and ventilation stages. In the initiation state, the pump injects a small amount of air (about 5 mL) into the sampler to push any condensation water out of the tube and to have
40 a starting pressure equivalent to the sensor detection limit. During the measurement state, bubbles are trapped in the funnel, the pressure signals are continuously monitored by the datalogger. When the pressure signal increases to a high level that signals that the bubbles have filled up the PVC pipe, the headspace of trapped bubbles can be either vented away or measured in a connected CH_4 and CO_2 sensor box. The controller activates a ventilation cycle in which the pump purges the trap, and then the valve opens for ventilation. The valve closes again when the pressure signal drops down to the initial
45 detection limit level. This also prevents water from entering the tube which could cause moisture blockage and a limited

sensor response. The ventilation stage cycles three times until the headspace is replaced by air. This measuring cycle (Figure 1) makes the ABC fully automated and operational over long periods - week to months or perhaps years given adequate power supply.

5   The pressure data can be recorded either to an SD card on the data logger or by wireless transfer to an onshore computer for subsequent transfer to a cloud in internet (See Section 3.3 Wireless network in Supplementary material). The data file is then processed (Matlab, etc) to extract the ebullition events from baseline noise based on the stepwise increase of the pressure signal. When the ABC was deployed in the field, the baseline noise increased. Even if the pressure sensor is pre-calibrated and has a temperature compensated range from 0 to 50°C, the weather conditions, including temperature, wind and waves,
10   will physically affect (shrink or expand) the bubble in the trap. Therefore, the noise removal is a critical procedure in data processing to extract the bubble events.

The regular electric noise, drift, and wind/wave effects on the pressure sensor generate high frequency low level signals. A bubble, on the other hand, will generate an abrupt jump that raises the level of pressure signal. In general, this leads to
15   periods with constant average pressure separated by a finite number of abrupt signal jumps to new levels due to bubbling. This reflects a piecewise constant signal (Little and Jones, 2011). The noise needs to be removed to identify the bubble events. The classical noise removal solvers, such as smoothing, or filtering over a moving window, have several limitations when the signal can abruptly change, and the abrupt changes of pressure signals need to be allocated and preserved. From our field measurement data, the noise, which generally are symmetric and tailed caused by temperature changes (Figure 1),
20   can be removed by the jump penalization method (Little and Jones, 2011). This jump penalization solver was chosen based on the observed results from 10 different noise removal solvers that were included in a "piecewise constant toolbox" (http://www.maxlittle.net/software/). This toolbox implements algorithms for noise removal from 1D piecewise constant signals, such as total variation and robust total variation denoising, bilateral filtering, K-means, mean shift and soft versions of the same, jump penalization, and iterated medians (Little and Jones, 2011). After the noises were removed, the denoised
25   data is composed of flat regions at different pressure levels and the boundary of those regions. The pressure levels are proportional to the volume of bubbles in the trap and the locations of the jumps are the time when bubbles enter the trap. These events were detected by applying point-wise (1st order) differentiation calculations on the denoised data. The positive differentiates, with peak heights greater than three times the standard deviation of the baselines, are identified as ebullition events. A report data file including date, time of the ebullition event and sizes of bubble are exported as a text file.

30   **2.2 Measuring CH$_4$ and CO$_2$ flux in an AFC with low cost sensors.**

The AFC system presented in Duc et al. (2013), was improved by equipping the floating chamber with the previously described low cost CH$_4$ and CO$_2$ sensors. To protect these sensors in high humidity environment, they were coated by polyurethane resin (e.g. arathane 5750 or Ultifil 3000-010, details are in Section 1.1 Sensor coating in Supplementary material). To prevent water splashing, the sensors were placed in a protected plastic box with holes for air through-flow that
35   is mounted in the chamber. A detailed design is described in Bastviken *et al.* (2015), however in this study the condensation protection sheet was not used. A rubber tube (230x65 mm Inner Tube Straight Valve Stem, Part # 952932367600, esska.se) was attached to the chamber to automatically open/close the chamber for ventilation or accumulation phase by inflating and deflating the tube, respectively.

40   The CH$_4$ sensor was configured as shown in Eugster and Kling (2012). It is powered with 5Vdc and its analog signals are recorded via the analog input of the datalogger board (Duc et al., 2013). The CO$_2$ sensor data, including CO$_2$ concentration, relative humidity and temperature, were transferred to the datalogger via an I2C connection. The CO$_2$ sensor is powered with 10Vdc. The CO$_2$ sensors which were used in this study were prepared as described in Bastviken et al. (2015). In the recorded data file, in addition to the time stamp and sensor data, there is a chamber open/close marker. This helps to identify the
45   accumulation and ventilation phases of the chamber. These data are post-processed with a script (written in Matlab, MathWorks, USA) to determine the fluxes during the chamber accumulation period.

Methane flux is determined based on the change of filtered CH_4 sensor signals over an accumulation period. The filter is set to select data period in which the variation of RH and temperature in the chamber are small enough to not affect CH_4 sensor signals. The diffusive flux is estimated from the best linear increase of CH_4 sensor signals without ebullition event. Additional details are presented in the CH_4 sensor calibration section. The CO_2 sensor was tested previously for use in flux

5   chambers to determine CO_2 emission (Bastviken et al., 2015). The slope of the CO_2 concentration linearly changing in the time range, which has r^2 higher than 0.98, is extracted as the rate of CO_2 emission per time. In our field study, the chamber is closed for 100 minutes and open about 20 minutes for ventilation, and data from the sensors was output every 1 minute. The GHG flux is calculated using the following equation.

$$F = \frac{\Delta C}{\Delta t} \frac{PV}{RT} \frac{60 * 10^{-6}}{A} \qquad \text{Eq. 1}$$

10   where F is flux (e.g. mol m^{-2} h^{-1}), $\Delta C/\Delta t$ is changing of GHG concentration over accumulation time in the FC headspace (ppmv min^{-1}), P is atmospheric pressure (atm), V is the FC volume (6300 mL), R is the gas constant (82.0562 mL atm K^{-1} mol^{-1}), T is the temperature (K), A is surface area of the FC (0.069 m^2), 60 is a conversion factor from min^{-1} to h^{-1} and 10^{-6} is a conversion factor from ppmv to mixing ratio measured in the gas. In this study, the $\Delta C/\Delta t$ (ppmv min^{-1}) is used to demonstrate the response of CH_4 and CO_2 sensors.

15   **2.3 CH$_4$ sensor test and calibration**

The responses of the CH_4 sensor to concentration, temperature and relative humidity (RH) in the chamber were studied, as well as, the effect of hydrogen sulfide (H_2S), which is a potential inference gas released from some sediments. On a water tank in the laboratory, the AFC was set to close on water surface for 100 minutes and open 20 minutes for ventilation. Water temperature was regulated at different temperatures from 10 to 35°C. In temperature sensitivity experiment, the starting CH_4

20   concentration was atmospheric levels (about 2 ppm), at which temperature were varied. In the calibration experiments, at different temperature levels, about 10 mL of CH_4 1000 ppm was injected into the 7 L chamber every 5 minutes until the AFC activates the ventilation process. About 5 minutes after the injection, a 10-mL gas sample from the chamber was withdrawn and injected into a gas chromatograph equipped with a flame ionization detector (GC-FID) to measure CH_4 concentration to be compared with sensor retrieved values. This test was repeated and, in later, the headspace gas in the chamber was

25   circulated through a spectrometric gas analyzer LGR (Los Gatos Research Inc.; DLT 100) for continuous CH_4 and CO_2 concentration measurements. The sensor test experiment was carried out with all three CH_4 sensor types mentioned above (TGS2611-E00, a factory calibrated CH_4 sensor module NGM 2611-E13 and the Panterra CH_4 sensor).

The H_2S interference experiment was carried out by injecting different volumes (from 2 to 637 mL) of standard gas H_2S 100

30   ppm (from Duotec AS, Denmark) into the test AFC. The chamber headspace gas was circulated through a Biogas analyzer (from Geotechnical Instrument, England) for measuring molecular oxygen (O_2) and H_2S. These results were analyzed using the JMP Pro software and Matlab to determine noise levels, quantitative flux determination limits, and a calibration equation.

2.4 Field deployment and monitoring

The field tests were performed on lakes at Stordalen Mire located in Abisko, Sweden (Wik et al., 2013). The floating control

35   box was tied to a buoy, which was anchored to the lake bottom. The funnel and the chamber were attached to the control box with distance of 0.5 and 1 m, respectively. The funnel and chamber were able to freely move around the anchor point in an area of about 2 m radius.

3. Results

3.1 Bubble counter calibration experiment

40   Calibrating the bubble counter revealed that the pressure sensor cannot detect the first 5 mL gas in the trap due to the low accumulation pressure (Figure S2). Therefore, to reach the detection limit of the pressure sensor, the automatic bubble

counter is started (prime pressurized) by pumping approximately 5 mL of air into the trap. This offset the ABC in every measurement cycle. At pressures above this low-end threshold, the pressure sensor response showed a linear response to the volume of the gas captured in the trap. The upper threshold for a volume change that the trap can detect depends on the length of the extension PVC pipe. The longer extension pipe, the wider linear range of the bubble counter. Therefore, the

5 ABC was programmed to end a bubble trap period by venting trapped gas before the extension pipe is completely filled with gas.

In stable conditions in the laboratory, the baseline noise of the bubble trap at all pressure levels in the linear calibration curve is approximately 0.013 V. The detection limit calculated from three times the noise (0.039 V) is equivalent to about 0.8 mL.

10 This means that our sensitivity is good enough to detect a bubble volume of 1ml that has high occurrence probability (Wik et al., 2013). In the post data processing, this detection limit was set to ignore any stepwise increase signal that is smaller than 0.04 V. Field deployment data and the processed signal from a pressure sensor used to extract the bubble events are shown in Figure 1. The pressure in the trap was affected by air temperature, especially the diel temperature cycle. If there is no bubble in the trap, the pressure signals fluctuate around a certain median value (Fig 2a). Small bubbles that enter the trap, do not

15 create a strong increasing stepwise signal that was easily distinguished relative to the background noise. However, small bubbles still raised the pressure signal median which can be detected by the jump penalization solver (Fig 2b). The larger bubbles (around 3 - 4 mL) made clear stepwise increases in the pressure signal beyond the background noise and the jump penalization solver was able to extract the median of this stepwise pressure level. Larger bubbles therefore were determined with better resolution. Two cycles of bubble accumulation over a long-term field deployment from two tested devices shows

20 that a wide variability of bubble sizes can enter the trap, from small bubble sizes (1 - 2 mL) who's signal is buried in the noise, to a large bubble (> 6 mL) that creates a large pressure signal compared to the background (Figure 2). If bubbles entered the trap and were large enough to activate the venting mechanism during a non-logging period, it was missed in the logged data file.

3.2 AFC CH_4 sensor calibration experiment

25 The response of the CH_4 sensor, when the chamber closed on water surface, to changing temperature, RH, and CH_4 concentration (around 2ppmv), is shown in Figure 3. In the first few minutes after chamber closure, the temperature and RH changed quickly in the chamber, causing a drift in the CH_4 sensor signal, but once temperature and RH stabilizes, the sensor responded in a predictable way to changes in CH_4 concentration inside the chamber. After temperature and RH stabilization occurred in the chamber, we determined the detection limit of our instrument for CH_4 fluxes based on the noise of the CH_4

30 sensor. In these blank experiments, the RH was always in the range of 60 - 90%, which is within the sensor RH operating range. The operation of the CH_4 sensor includes heating it to a high temperature to detect combustible gases, therefore, the temperature inside the sensor box is always higher than the water temperature. The temperature sensor of the ELG CO_2 sensor measured the changing of temperature inside the sensor box over the water temperature. The noise over a whole accumulation period (100 minutes) was about 2.44 ± 1.21 mV. A minimum accumulation rate limit is calculated as five

35 times the noise or about 12.2 mV. Therefore, we calculated the CH_4 concentration increase that generated a CH_4 sensor signal of 12.2 mV to be equivalent to 5.25 ppm and used this to calculate a minimum detectable CH_4 flux. In an accumulation period, the accumulation rate detection limit of this sensor embedded in the chamber is 5.25 ppm per 100 minutes (0.0525 ppm per minute).

40 At all temperatures (10, 20, 25 and 30°C), the three CH_4 sensor signals were well correlated to CH_4 concentration however, these correlation lines have different intercepts depending on water temperature (Figure S3 a-c). The absolute concentrations measured by the sensors were affected by temperature and RH and were not suitable for use. To study CH_4 flux, we instead used the relative change of CH_4 concentration over time from five minutes after chamber closure to avoid the periods with the largest changes in temperature and RH. Accordingly, the differential CH_4 sensor signal (d0_CH4sens), which is the

45 difference between the current measurement and the initial measurement point 5 minutes after the chamber closed on water surface, was used instead of the raw output signal from the sensor. Indeed, the differential CH_4 sensor signal was less sensitive to temperature and had a linear response ($r^2 = 0.98$; $p < 0.001$) across the studied temperatures (Figure 4). In this test, the variability in the temperature and RH were in ranges of 2°C and 5%, respectively, while CH_4 concentration

increased from atmospheric or about 2 ppm to 25 ppm. The standard least square fit model was applied on d0_CH4sens as a model response and the changing CH_4 concentration, temperature and RH as model effects. The result showed that the variability of temperature (p = 0.038) and RH (p = 0.867), have less significant effects on the CH_4 sensor response compare to the contribution of CH_4 concentration (p_value < 0.001). This reveals that these CH_4 sensors can be used to measure CH_4 flux when the temperature and RH conditions are stable in the chamber.

The effect of temperature and RH can be corrected for in the response of the sensor using an algorithm developed by Eugster and Kling (2012), but this was not applied in our study because we were not able to simulate the natural variations of outdoor temperature and RH conditions on our control experiment. Therefore, periods with stable temperature and RH were used and the calibration curve for the TGS2611-E00 CH_4 sensor in our application was the average linear response of d0_CH4sens versus the changing of CH_4 concentration (d0_CH4conc) without temperature and RH correction (Figure 4)

$$d0\_CH_4sens = 1.256 \times d0\_CH_4conc + 5.871 \qquad \text{Eq. 2}$$

where d0_CH4sens is the voltage change of the CH_4 sensor in mV, and d0_CH4conc is in ppmv. Comparing with this sensor, calibration results showed that the pre-calibrated Figaro NGM2611-E13 module has about the same response to the change in CH_4 concentration at all temperatures. The NGM2611-E13 had a regression equation as following:

$$d0\_CH_4sens = 1.116 \times d0\_CH_4conc + 1.771 \qquad \text{Eq. 3}$$

The Panterra CH_4 sensor showed a different response at different temperatures (Figure 4). Its calibration lines had different response at 10 and 15°C, and its d0_CH4sens has negative response when d0_CH4conc is higher than 15 ppm at 20 and 30°C.

In the H_2S interference test, the injected volume of H_2S standard increased from 2 to 637 mL. The Biogas analyzer did not detect any H_2S even when the estimated H_2S concentration in the chamber was 9 ppm. This level is close to the detection limit of the instrument, and given the minimum analytical uncertainty of ± 10 ppm, it is likely that H_2S was present in high enough amounts to affect the CH_4 sensors. During the H_2S addition, the CH_4 sensor signal increased to more than 5 times of baseline noise; therefore, H_2S was considered to affect the sensor response, in agreement with sensor producer tests.

3.3 CH4 and CO2 flux with the AFC

The pilot field deployment of the AFC embedded CH_4 and CO_2 sensors showed that the system was effective for measuring the variation of CH_4 and CO_2 concentration in the chamber over time (Figure 5 a-c). The automatic mechanism developed to close the chamber for flux measurements and open the chamber for ventilation periods/phases helped to reduce condensation and allowed for a linear response of the CO_2 sensor (Figure 5b). This is an improvement over past work and allows for the sensor to be deployed in the field for long time periods. There was a situation when the chamber was closed on water surface for a whole night due to a low-battery. As a result, the saturated RH in the chamber became higher than 100% and caused condensation and malfunction in the sensor until drying (discussed in Bastviken et al. 2015). After two ventilation cycles, the CO_2 sensor dried and the baseline decreased to the normal linear response range. The CO_2 sensor responses were not affected by temperature and RH in our experiment. Therefore, CO_2 flux is determined from the slope of the best linear response data in an accumulation period.

During measurement periods, right after ventilation, CO_2 concentrations in the chamber are supposed to be equal to the atmospheric CO_2 concentration above the lake surface. These initial CO_2 concentrations varied within a range of 516 - 1179 ppmv with higher mixing ratios during nighttime. Because the chamber ventilation time was early in the development adjusted to allow complete ventilation of the chamber headspace, the elevated starting concentrations may reflect actual concentrations if stable atmospheric conditions resulted in a buildup of CO_2 released from the lake and surrounding mire ecosystem.

The field deployments revealed that there were many periods in which temperature and RH conditions of the chamber were stable enough (Figure 5a) for the Figaro CH_4 sensors to adequately measure the changing of CH_4 mixing ratio in the chamber. In cases where temperature and RH varied a lot, the data processing script determined periods of data where the variation of temperature and RH was less than 2°C and 5%, respectively, defining periods for which CH_4 sensor data could be reliably evaluated. If ebullitive CH_4 entered the chamber headspace, there was a clear positive change in the sensor signal output. This was easily identified as a stepwise increase of the CH_4 sensor signal over a very short time. This signal identified the type of ebullitive flux that could be measured over that chamber closure period. For diffusive CH_4 flux measurements, the d0CH4sens data, with a sensor response of less than 30 mV (within linear calibration range) and without a stepwise jump, were scanned for a data range with best linear adjusted R square. For diffusive flux estimation, the $\Delta C/\Delta t$ (ppmv min^{-1}) in Eq. (1) is calculated using the last d0CH4sens point in this linear range, in which d0CH4sens is converted to d0 CH_4 concentration (ppmv) follow Eq. (2) and its coordinate in time since the chamber closed is calculated the measurement period (minute). The manually collected gas samples in the field and the CH_4 mixing ratio change over time (ppmv/time) in the chamber headspace determined from the sensor response showed a strong linear relationship with a deviation less than 15% (Figure 6). The ebullitive CH_4, which detected by the CH_4 sensor in the FC, was not concentration quantified in this study focusing on the relative changes of the methane sensor in the low range, because CH4 sensor response to ebullition events was usually out of the linear calibration range.

4. Discussion

4.1 Automated ebullition measurements using pressure sensors

Deploying pressure sensors to determine the timing of ebullition events and to measure the bubble volumes has been thoroughly tested by Varadharajan et. al. 2010. Our bubble trap introduces a way to automatically reset after being full of gas that allows for long-term deployment with minimum maintenance effort. Further, via the jump penalization noise removal method, bubble events can be detected despite the noise caused by changes in air temperature affecting the differential pressure and therefore bubble volumes. It is however important that the ABC is gas tight. This is not a simple requirement; especially because the trap is built from plastic materials meant to be easily disconnected for portability and is exposed to the outdoor environment. After a long deployment time, leaks were occasionally observed at the assemble joint of the pressure sensor. So far, if a trap leak happens, the pressure is lower than the priming pressure threshold, which was set to trigger a warning indication to the host server controller on the lakeshore. It can be fixed by applying silicone glue on the leak site. For a long term solution, the recent study using optical sensors in an open path funnel (Delwiche and Hemond, 2017) suggests an alternative and interesting design for ebullition studies, which could be combined with the present sensor approach to also quantify CH4 content in the bubbles.

4.2 Automatic measurement of CH_4 and CO_2 during chamber fluxes

In our application, the low cost CH_4 and CO_2 sensors can be used to log changing CH_4 and CO_2 concentrations. It is a direct approach to measure CH_4 and CO_2 flux from a defined-footprint area on the time scale of minutes-hours, extending over long-time periods given a suitable power supply. The chamber captures both ebullition and diffusion fluxes. Ebullition events are marked by abrupt changes in the response of the CH_4 sensor and therefore can be identified readily. The diffusive flux is identified by the gradual change in CH_4 and CO_2 concentration over time. We did observe ebullition events in the chamber during deployment periods, in support of the previous indications that ebullition typically accounts for a large share of the open water flux (Figure 5c). However, since the sensor is not calibrated for very high concentrations, we could not determine the flux rate observed during these events. This remains a challenge for future work.

To study diffusive fluxes, it is important to measure the change of gas concentrations during a short period of time right after the chamber closes. This requires a gas sensor that can measure at near ambient gas concentrations. The CH_4 injection experiment showed that both of the Figaro CH_4 sensors have sensitivity at low ppm mixing ratios and yield a linear response

from ambient at about 2 ppm up to 25 ppm. The TGS2611-E00 and NGM2611-E13 have small differences in their response (slope) in the linear range, however, their responses to experimental conditions are identical because they use the same sensor base. It is possible that the sensors can be used outside the range reported here by calibrating with another response curve. In any case, we recommend to adjusting the AFC accumulation time to the effective range of the sensor.

5   Alternatively, flux calculation can be based on data within the linear range only in the post-processing of the data. Calibration for the Figaro CH_4 sensor is recommended for each individual sensor. The response slopes of different sensors could deviate up to 12%. For practical reasons, if flux estimation with tolerance ±20% error (arbitrary range of high accuracy) (Wik et al., 2016a) is accepted, one general calibration line can be obtained from a calibration of at least five CH_4 sensors for statistical representativeness. In our study, the calibration line is obtained from the calibration experiment of

10   eight sensors. Due to the effect of temperature and RH, the calibration curve should be based on calibration data at different water temperatures that cover anticipated field conditions. Compared to Duc et al., 2012 which used the Panterra CH_4 sensor, the Figaro CH_4 sensor gives a better flux measurement result in field conditions. The Panterra CH_4 sensor signal has been compensated for the temperature effect, but is probably not applicable for temperatures lower than 15°C.

15   The H_2S interference test revealed that H_2S, a corrosive gas which can be released from anoxic sediments in sulfur rich systems, may interfere with sensor response. Therefore, extra care and thorough data validation is suggested when applying the sensors in sulfur rich environments. In additions, this CH_4 sensor responses based on reaction between O_2 in air and reductant (flammable) gases; therefore, any change in concentrations of either O_2 or reductant gases could contribute to the signal of the sensor. This CH_4 sensor can combust a small amount CH_4 gas (about 0.0041 ppmv per minute), this needs to be

20   considered when the CH_4 flux is low (near the detection limit 0.0525 ppmv per minute of this sensor in our application) and chamber accumulation time is very long.

One limitation of the CH_4 sensor is its power consumption. While the CO_2 sensor can be activated once per minute (or at other desired time intervals), the CH_4 sensor needs to be heated at all times. In our case, these systems were deployed at high

25   latitudes in the summer and the battery was recharged by a 13W solar panel. If the weather was cloudy for four to five days in a row, the battery voltage decreased below 10.5 V. The system automatically turns off until the battery is recharged. In 2017, the replacement lithium ion battery 12V 55Ah (Power Pack LS 55) helped to keep the system working continuously during longer time periods and reduced the weight of control box.

30   Over our deployment time, there were several chambers that were either submerged or turned over. The chambers were submerged because the rubber inner tube degraded due to UV exposure over a long period of time, generally two sampling seasons. This problem was solved by covering the inner tube with aluminum foil or by changing to the gas delivery flow scheme shown in Figure S7. With this new flow design, there is no underpressure built up in the chamber during the ventilation process; even in a situation where the chamber cannot open due to failure of the rubber inner tube. With this

35   configuration, the sample array presented in Duc et al (2013) cannot be used. The strong correlation between grab samples and the sensors (Figure 5) allow us however to capture the high temporal fluxes and skipping the labor intensive process of analyzing grab samples. The grab samples can however be taken periodically as a cross check of the sensor response. The other problem of chamber flipping probably was caused by wind suddenly change its direction during chamber ventilation process. The opening chamber picked the wind and flip over before the AFC-ABC system could be reoriented follow wind

40   direction. To prevent this flipping, the opening side of the chamber were attached with two floating anchors (called anti-flipping anchor) (Figure S8). With this improvement, so far, there has been no chamber flip during tests with maximum wind speed up to about 7 m/s.

4.3 Challenges when networking measurement systems remotely

45   In our study, the traps were on the lake surface which was usually lower than ground level and surrounded by tree and plants. Over the study season, the growth of vegetation on the lakeshore can potentially block the line-of-sight between the host controller and the traps on the lake, which can hamper radio communication. To guarantee radio communication, at least one client (i.e. chamber system) was placed in a strategic place which had a clear line of sight to the host controller. Within the

digimesh network, XBee modules can form a self-configuring, self-healing wireless peer-to-peer network with other data loggers in radio range. Therefore, the host controller doesn't necessarily need to have direct line-of-sight communication with all of the traps on the lake surface. If some of the traps are out of the controller's direct range, they should be automatically passing their messages through closer clients. Therefore, it is important to keep a robust network topology.

5

Errors within this network still occur every once in a while, probably due to high humidity environment around the clients and variations of weather conditions, temperature and humidity (Luomala and Hakala, 2015). This could cause failure in transfer of some initial data packet in the data file, or break the communication with clients. Hence, software for this system was developed to address these errors. For example, all the data packets were encoded, so the missing data can be easily

10 identified in the post data processing and the host controller keeps searching to reestablish communication with "lost" clients. Detail of wireless communication protocol and host-controller design are presented in Supplementary material.

5. Conclusions

Resolving diffusive and ebullitive GHG fluxes at the air-water interface in a well-defined footprint area is needed so that we can accurately represent open water bodies likes lakes and streams in global CH_4 and CO_2 budgets. Any measurement has to

15 preserve the robustness of using chambers and funnels as the traps to capture these fluxes. With the benefit of low cost technology, we have modified these simple traps to function automatically with wireless remote monitoring and control via an internet browser. These traps are equipped with not only the sensors to monitor the fluxes in high temporal resolution but also the electro-mechanical hardware to do complex actions in the field such as venting traps and collecting gas samples (if needed). This is our first attempt to integrate several low-cost technologies to make a device to measure GHG emissions

20 from lakes with the data updated online in real time. This device, as an open source technology for non-profit academy study, can hopefully contribute to studies of GHG emission from aquatic environments in remote and logistically difficult areas.

Code availability

25 Software to setup a webserver on a Raspberry pi computer and C code to program the microchip of an Xbee datalogger will be kept updating and published at. DOI: http://dx.doi.org/10.17632/yb4h7p4xp4.2

Data Availability

Supplement link

30 (from Copernicus)

Author contributions.

NTD: hardware, software designed the AFC-ABC system, conducted the study, developed Matlab script and processed data and co-wrote the manuscript; SS: hardware, core-software designed the wireless datalogger, webserver and contributed to the manuscript; MW conducted the study and contributed to the manuscript; PC, DB, RKV gave advice through all the study

35 and co-wrote the manuscript. All authors discussed the results and commented on the manuscript.

Competing interests.

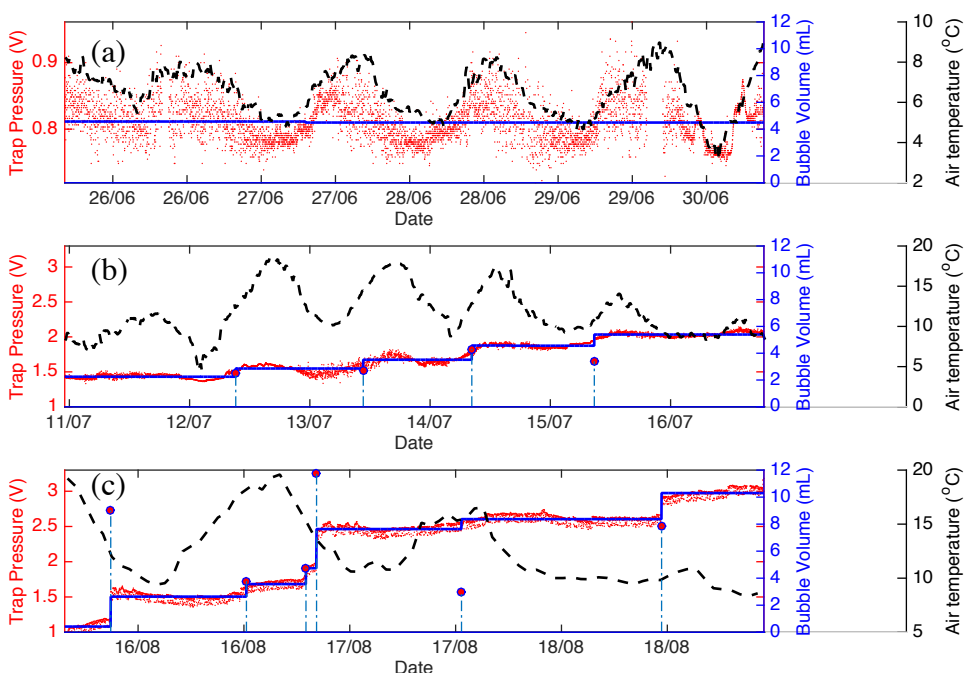The authors declare that they have no conflict of interest.

10   **References**

Anderson, D. E., Striegl, R. G., Stannard, D. I., Michmerhuizen, C. M., McConnaughey, T. A., and LaBaugh, J. W.: Estimating lake-atmosphere CO2 exchange, Limnol. Oceanogr., 44, 988-1001, 10.4319/lo.1999.44.4.0988, 1999.

Bastviken, D., Cole, J., Pace, M., and Tranvik, L.: Methane emissions from lakes: Dependence of lake characteristics, two regional assessments, and a global estimate, Global Biogeochem. Cycles, 18, GB4009, doi:4010.1029/2004GB002238., 10.1029/2004GB002238, 2004, 2004.

Bastviken, D., Tranvik, L. J., Downing, J. A., Crill, P. M., and Enrich-Prast, A.: Freshwater Methane Emissions Offset the Continental Carbon Sink, Science, 331, 50, 10.1126/science.1196808, 2011.

Bastviken, D., Sundgren, I., Natchimuthu, S., Reyier, H., and Gålfalk, M.: Technical Note: Cost-efficient approaches to measure carbon dioxide (CO 2) fluxes and concentrations in terrestrial and aquatic environments using mini loggers, Biogeosciences Discuss., 12, 2357-2380, 2015.

Chanton, J. P., and Whiting, G. J.: Trace gas exchange in freshwater and coastal marine environments: ebullition and transport by plants., in: Biogenic Trace Gases: Measuring Emissions from Soil and Water, edited by: Matson, P. A., and Harriss, R. C., Wiley-Blackwell, Oxford, 98-125, 1995.

Cole, J. J., Bade, D. L., Bastviken, D., Pace, M. L., and Bogert, M. V. d.: Multiple approaches to estimating air-water gas exchange in small lakes, Limnol. Oceanogr. Methods, 8, 285-293, 10.4319/lom.2010.8.285, 2010.

Delwiche, K., and Hemond, H. F.: An enhanced bubble size sensor for long-term ebullition studies, Limnol. Oceanogr. Methods, 15, 821-835, 10.1002/lom3.10201, 2017.

Downing, J. A., Prairie, Y. T., Cole, J. J., Duarte, C. M., Tranvik, L. J., Striegl, R. G., McDowell, W. H., Kortelainen, P., Caraco, N. F., Melack, J. M., and Middelburg, J. J.: The global abundance and size distribution of lakes, ponds, and impoundments, Limnol. Oceanogr., 51, 2388–2397, 2006.

Duc, N. T., Silverstein, S., Lundmark, L., Reyier, H., Crill, P., and Bastviken, D.: Automated Flux Chamber for Investigating Gas Flux at Water–Air Interfaces, Environ. Sci. Technol., 47, 968-975, 10.1021/es303848x, 2013.

Eugster, W., and Kling, G. W.: Performance of a low-cost methane sensor for ambient concentration measurements in preliminary studies, Atmos. Meas. Tech., 5, 1925-1934, 2012.

Gålfalk, M., Bastviken, D., Fredriksson, S., and Arneborg, L.: Determination of the piston velocity for water-air interfaces using flux chambers, acoustic Doppler velocimetry, and IR imaging of the water surface, Journal of Geophysical Research: Biogeosciences, 118, 770-782, 10.1002/jgrg.20064, 2013.

Goodrich, J. P., Varner, R. K., Frolking, S., Duncan, B. N., and Crill, P. M.: High-frequency measurements of methane ebullition over a growing season at a temperate peatland site, Geophys. Res. Lett., 38, L07404, 2011.

Goulden, M. L., and Crill, P. M.: Automated measurements of CO2 exchange at the moss surface of a black spruce forest, Tree Physiology, 17, 537-542, 10.1093/treephys/17.8-9.537, 1997.

Johnson, M. S., Billett, M. F., Dinsmore, K. J., Wallin, M., Dyson, K. E., and Jassal, R. S.: Direct and continuous measurement of dissolved carbon dioxide in freshwater aquatic systems—method and applications, Ecohydrology, 3, 68-78, 10.1002/eco.95, 2010.

Little, M. A., and Jones, N. S.: Generalized methods and solvers for noise removal from piecewise constant signals. I. Background theory, Proc. Math. Phys. Eng. Sci., 467, 3088-3114, 10.1098/rspa.2010.0671, 2011.

Lorke, A., Bodmer, P., Noss, C., Alshboul, Z., Koschorreck, M., Somlai, C., Bastviken, D., Flury, S., McGinnis, D., and Maeck, A.: Technical Note: Drifting vs. anchored flux chambers for measuring greenhouse gas emissions from running
5   waters, Biogeosciences Discuss., 12, 2015.

Luomala, J., and Hakala, I.: Effects of Temperature and Humidity on Radio Signal Strength in Outdoor Wireless Sensor Networks, Acsis-Ann Comput Sci, 5, 1247-1255, 10.15439/2015f241, 2015.

Marotta, H., Pinho, L., Gudasz, C., Bastviken, D., Tranvik, L. J., and Enrich-Prast, A.: Greenhouse gas production in low-latitude lake sediments responds strongly to warming, Nature Clim. Change, 4, 467-470, 10.1038/nclimate2222, 2014.

10 Meng, L., Hess, P. G. M., Mahowald, N. M., Yavitt, J. B., Riley, W. J., Subin, Z. M., Lawrence, D. M., Swenson, S. C., Jauhiainen, J., and Fuka, D. R.: Sensitivity of wetland methane emissions to model assumptions: application and model testing against site observations, Biogeosciences, 9, 2793 - 2819, 2012.

Ostrovsky, I., McGinnis, D. F., Lapidus, L., and Eckert, W.: Quantifying gas ebullition with echosounder: the role of methane transport by bubbles in a medium-sized lake, Limnol. Oceanogr. Methods, 6, 105-118, 2008.

15 Raymond, P. A., Hartmann, J., Lauerwald, R., and Sobek, S.: Global carbon dioxide emissions from inland waters, Nature, 10.1038/nature12760, 2013.

Smith, S. V.: Physical, chemical and biological characteristics of CO_2 gas flux across the air-water interface, Plant Cell Environ., 8, 387-398, 10.1111/1365-3040.ep11660734, 1985.

Tassin, A. L., and Nikitopoulos, D. E.: Non-intrusive measurements of bubble size and velocity, Exp. Fluids, 19, 121-132,
20 1995.

Tranvik, L. J., Downing, J. A., Cotner, J. B., Loiselle, S. A., Striegle, R. G., Ballatore, T. J., Dillon, P., Finlay, K., Fortino, K., Knoll, L. B., Kortelainen, P. L., Kutser, T., Larsen, S., Laurion, I., Leech, D. M., McCallister, S. L., McKnight, D. M., Melack, J. M., Overholt, E., Porter, J. A., Prairie, Y., Renwick, W. H., Roland, F., Sherman, B. S., Schindler, D. W., Sobek, S., Tremblay, A., Vanni, M. J., Verschoor, A. M., von Wachenfeldt, E., and Weyhenmeyera, G. A.: Lakes and reservoirs as
25 regulators of carbon cycling and climate, Limnol. Oceanogr., 54, 2298-2314, 2009.

Verpoorter, C., Kutser, T., Seekell, D. A., and Tranvik, L. J.: A global inventory of lakes based on high-resolution satellite imagery, Geophys. Res. Lett., 41, 6396-6402, 10.1002/2014gl060641, 2014.

Walter, B. P., Heimann, M., and Matthews, E.: Modeling modern methane emissions from natural wetlands 1. Model description and results, J. Geophys. Res. Atmos., 106, 34189-34206, 2001.

30 Wik, M., Crill, P. M., Varner, R. K., and Bastviken, D.: Multiyear measurements of ebullitive methane flux from three subarctic lakes, J Geophys Res-Biogeo, 118, 1307-1321, 10.1002/jgrg.20103, 2013.

Wik, M., Thornton, B. F., Bastviken, D., Uhlbäck, J., and Crill, P. M.: Biased sampling of methane release from northern lakes: A problem for extrapolation, Geophys. Res. Lett., 43, 1256-1262, 10.1002/2015GL066501, 2016a.

Wik, M., Varner, R. K., Anthony, K., MacIntyre, S., and Bastviken, D.: Climate-sensitive northern lakes and ponds are
35 critical components of methane release, Nature Geosci., 9, 99-105, 10.1038/ngeo2578, 2016b.

Yvon-Durocher, G., Allen, A. P., Bastviken, D., Conrad, R., Gudasz, C., St-Pierre, A., Thanh-Duc, N., and del Giorgio, P. A.: Methane fluxes show consistent temperature dependence across microbial to ecosystem scales, Nature, 507, 488-491, 10.1038/nature13164, 2014.

40

Figure 1: ABC pressure signal and air temperature over three field deployment periods. Red dots are trap pressure signals, blue lines are the denoised pressure sensor signal, stem plots (vertical dashed lines with red circle on top) are bubble events which were detected from the stepwise increase of denoised signals, and black dash plots are air temperature. (a) Sample period with no bubbles entering the trap, (b) Sample period with small bubbles entering the trap and (c) Sample period with both big and small bubbles entering the trap.

Figure 2: Two measurement periods of an ABC deployed in Mellersta Harrsjön, Stordalen, Abisko, 2015. (a and c) Sample period when bubbles entering the trap were detected from the denoised pressure signal. (b and d) air temperature and atmospheric pressure from an onshore weather station during the same sample period.
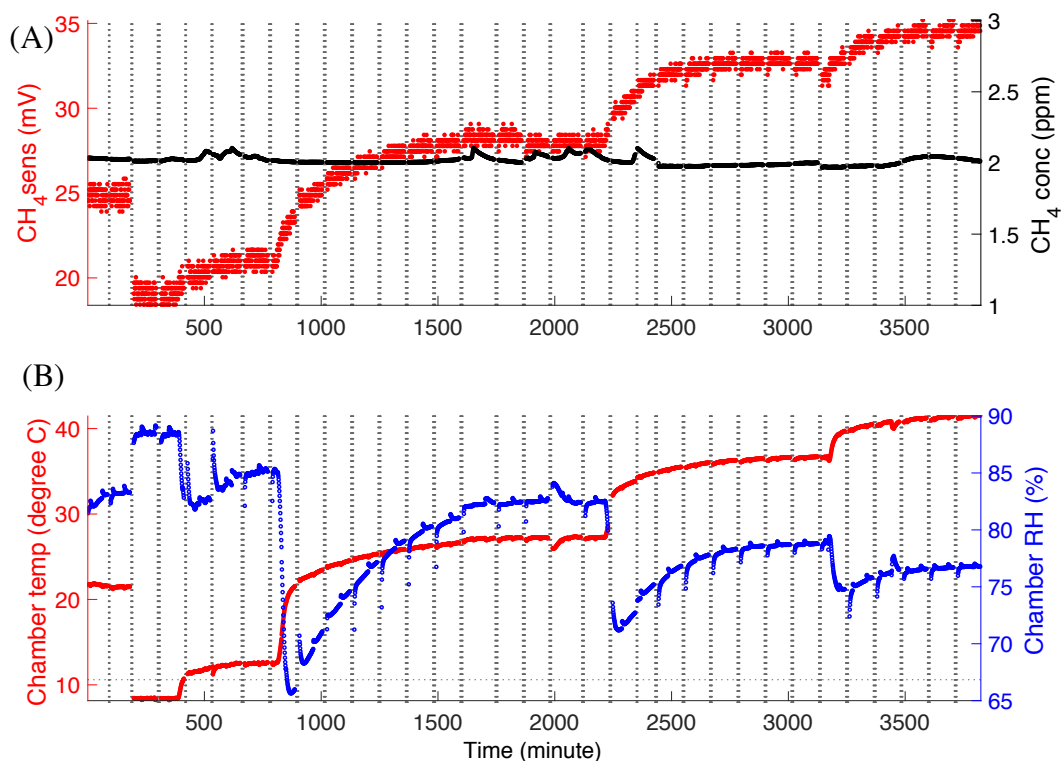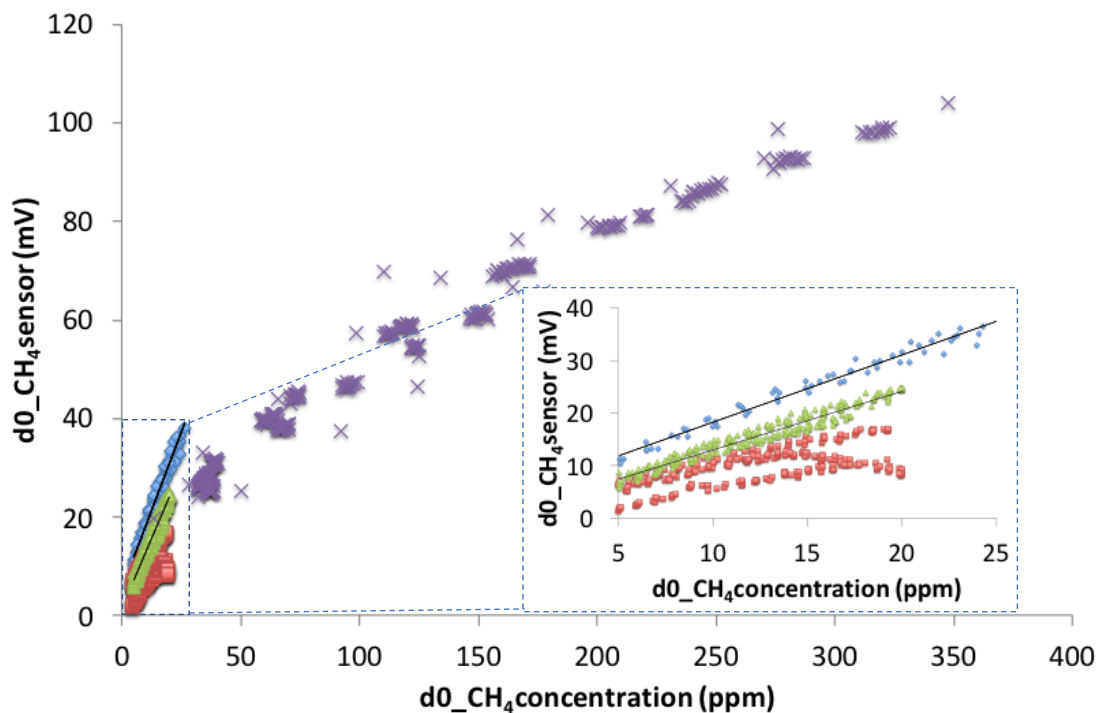
5

10

15

Figure 3: Methane (mV response and concentration), temperature (°C), RH (%) sensor responses in the initial phase of the sensor test experiment in which temperature of water tank was regulated in range from 5 to 35°C. A) CH4 sensor signal and actual CH4 concentration around 2ppm, and B) Temperature and RH in the chamber over the experimental period. Vertical dotted lines denote periods when chamber was opened for ventilation.

Figure 4: Calibration curves of the CH₄ sensors at all experimental water temperatures from 10 to 30°C. The blue diamonds, green triangles and purple crosses (Δ, x: for CH₄ concentration higher than 25 ppm), and red squares represent the change in the CH₄ sensor signal over time from the chamber closure (d0_CH4sens) of the TGS2611-E00, NGM2611-E13 and the Panterra sensor, respectively.
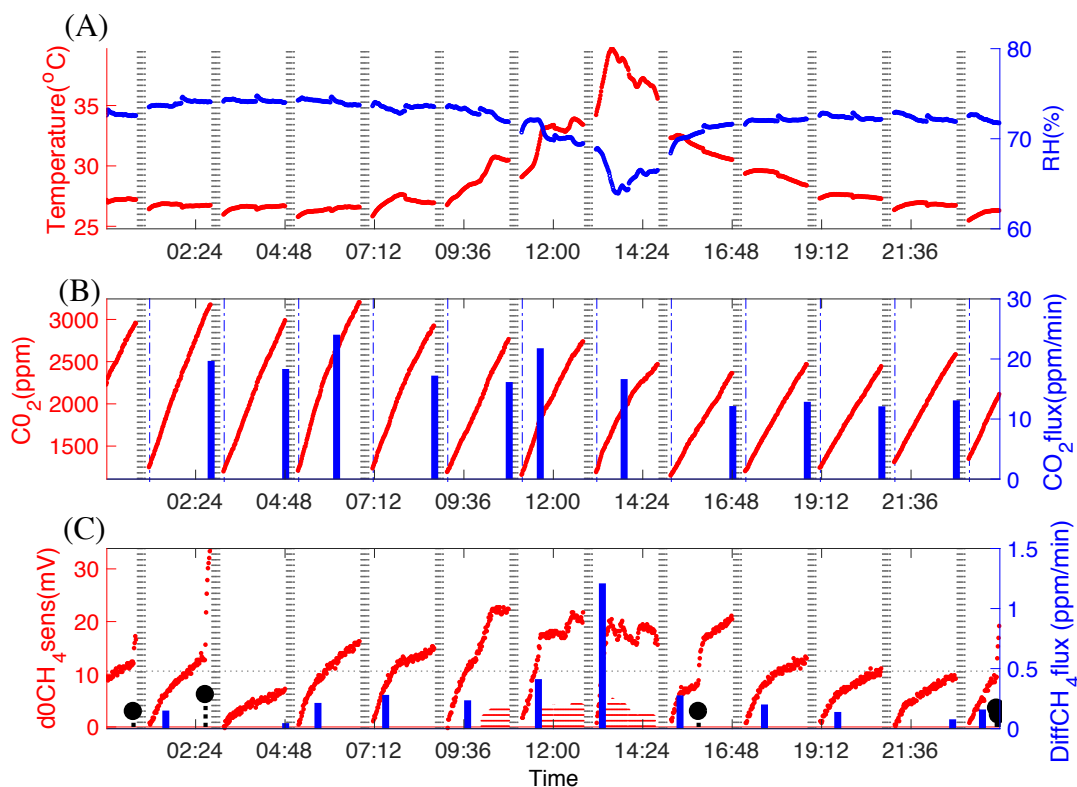
Figure 5: Example of one day of automatic flux chamber (AFC) measurements covering 11 accumulation periods. (A) scatter plot of temperature (left axis, red) and RH (right axis, blue) in the chamber. (B) scatter plot of CO_2 concentration measured by ELG CO_2 sensor (left axis) and bar plot of CO_2 fluxes calculated from slopes of the changing CO_2 concentration in time range marked from the vertical dash dot line to bar plot location (right axis). (C) scatter plot of CH_4 sensor signal (left axis) and bar plot of CH_4 fluxes (right axis) calculated from the best linear data range when d0CH4sens values are in the calibration linear range (less than 30 mV), temperature and RH changes are less than 2°C and 5%. Red shaded periods indicate sampling when temperature and RH are affecting the gas sensor response and therefore these data are not used in the flux calculation. In the event of an ebullition event, the flux calculation is made with data taken prior to that event. Ebullition events are marked by the black stem plot.
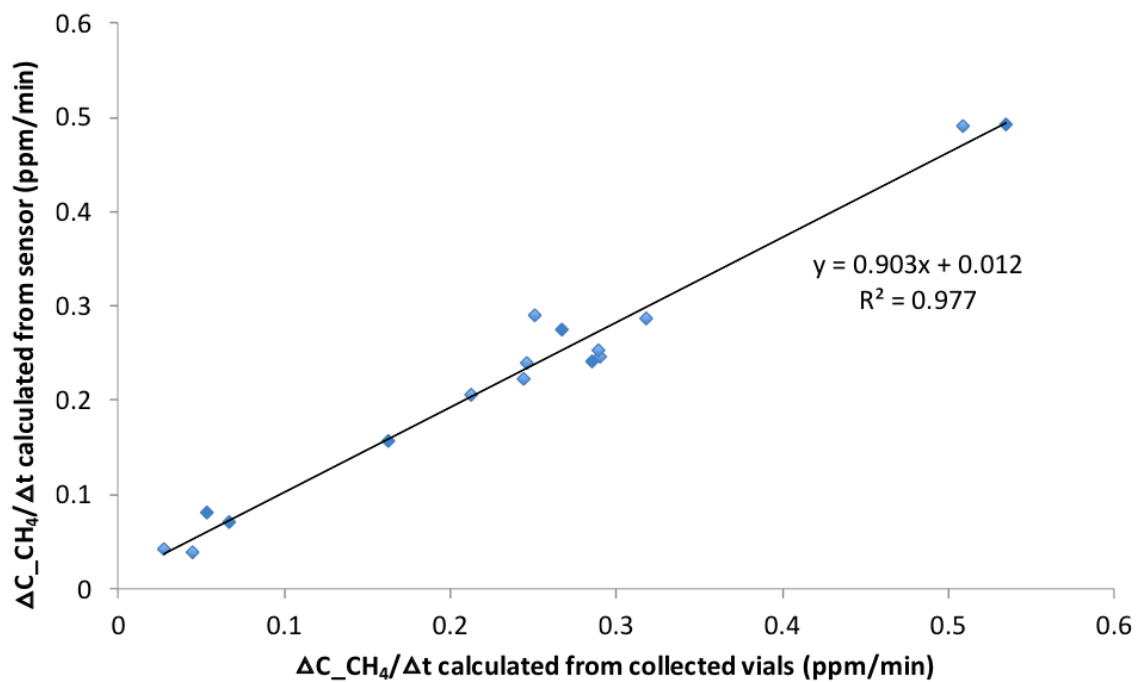
Figure 6: Methane accumulation rates calculated from an NGM2611-E13 CH₄ sensor signal compared to accumulation rates calculated from CH₄ mixing ratio in gas samples collected at the start and end of accumulation periods.

5

10

15